

Luminescence emission originating from nitrogen doping of β -Ga₂O₃ nanowiresY. P. Song,¹ H. Z. Zhang,¹ C. Lin,² Y. W. Zhu,¹ G. H. Li,³ F. H. Yang,³ and D. P. Yu^{1,*}¹*School of Physics, National Key Laboratory of Mesoscopic Physics, and Electron Microscopy Laboratory, Peking University, Beijing 100871, People's Republic of China*²*Spex Fluorescence Jobin Yvon, Inc., Edison, New Jersey 08820, USA*³*Semiconductor Institute, Chinese Academic of Sciences, Beijing 100083, People's Republic of China*

(Received 9 September 2003; published 10 February 2004)

Nitrogen-doped β -Ga₂O₃ nanowires (GaO NWs) were prepared by annealing the as-grown nanowires in an ammonia atmosphere. The optical properties of the nitrogen-doped GaO NWs were studied by measurements of the photoluminescence and phosphorescence decay at the temperature range between 10 and 300 K. The experimental results revealed that nitrogen doping in GaO NWs induced a novel intensive red-light emission around 1.67 eV, with a characteristic decay time around 136 μ s at 77 K, much shorter than that of the blue emission (a decay time of 457 μ s). The time decay and temperature-dependent luminescence spectra were calculated theoretically based on a donor-acceptor pair model, which is in excellent agreement with the experimental data. This result suggests that the observed novel red-light emission originates from the recombination of an electron trapped on a donor due to oxygen vacancies and a hole trapped on an acceptor due to nitrogen doping.

DOI: 10.1103/PhysRevB.69.075304

PACS number(s): 78.67.-n, 61.46.+w, 68.65.-k, 78.47.+p

I. INTRODUCTION

Monoclinic gallium oxide (β -Ga₂O₃) is a promising oxide semiconductor with the widest band gap (\sim 4.8 eV) to date,¹⁻⁷ which allows tunability in the wavelength range from infrared to ultraviolet for optical devices. For example, proper element doping can modify the electronic structure of the Ga₂O₃ and introduce defect levels between the band gap, which enable tunable light emissions. The β -Ga₂O₃ semiconductors have been widely studied not only for their high stability and tunability in optical properties, but also for their applications in high sensitive gas sensors working at high temperature^{1,8} and transparent conductors in optoelectronics.² Recently, nanostructure materials have been a focus of research for both fundamental physics and potential applications in nanoscale optoelectronic devices. Because of their high surface/volume ratio, Ga₂O₃ nanostructures are obviously preferable for many applications, such as surface-control-type gas sensors with very low energy expense. In particular, it was found that dopants or impurities in gallium oxide will considerably increase its conductance,⁹ and in turn modulate its optical properties.⁶ Bulk β -Ga₂O₃ crystal can exhibit ultraviolet (uv) and blue-green (BG) emissions. However, the luminescence origin of β -Ga₂O₃ nanowires (GaO NWs) is not well understood. Also, most of investigations on the luminescence focused on the gallium oxide powder or crystallites,^{6,7,10,11} and there were only a few works¹²⁻¹⁴ reported on the luminescence of GaO NWs. In this paper, β -Ga₂O₃ nanowires were doped with nitrogen prepared by annealing the as-grown nanowires in ammonia atmosphere, and the luminescence properties were investigated by photoluminescence measurements. The calculated time decay and temperature dependence of the luminescence agreed well with the experimental data.

II. EXPERIMENT

GaO NWs were first synthesized by Zhang *et al.* via vapor phase growth.¹ The GaO NWs used here were prepared

by the following method.¹ One hundred milligram metallic gallium was put on a silicon substrate and placed into a quartz boat. Two or three silicon substrates (110) deposited with a 5-nm Au film were placed downstream of the boat. The boat was then put into the center of an alumina tube (6 cm \times 100 cm), which was inserted in a horizontal tube furnace. The alumina tube was evacuated by a mechanical pump and cleaned by the flowing argon. The furnace was heated to 900 $^{\circ}$ C at a rate of 15 $^{\circ}$ C/min and kept for 30 min for nanowire growth with a flow of argon at 80 sccm. Afterwards, the temperature was decreased to 700 $^{\circ}$ C and kept for 30 min for nitrogen doping in flowing ammonia (50 sccm). When naturally cooled to room temperature in flow argon (80 sccm), a white layer material was observed on the substrates.

The morphology and microstructure of the products were characterized using transmission electron microscope (TEM, Tecnai F30) and field emission scanning electron microscopy (SEM). The chemical composition and dopant concentration were analyzed using x-ray photoelectron spectroscopy (XPS) and electron-energy-loss spectroscopy (EELS). Photoluminescence (PL) spectra were measured by a He-Cd laser with a 325-nm line in a temperature range between 10 and 300 K.

The as-grown GaO NWs were doped under flowing ammonia (50 sccm) atmosphere and the nitrogen concentration can be controlled by the temperature and the heating time. It was found that the higher the temperature and the longer the doping time, the more the nitrogen can be doped into the GaO NWs. Three representative samples were prepared for different dopant concentration (named sample no. 1, 700 $^{\circ}$ C/20 min; sample no. 2, 700 $^{\circ}$ C/40 min; and sample no. 3, 750 $^{\circ}$ C/40 min). The general morphology and microstructure of the N-doped GaO NWs (sample 1) are shown in the SEM [Fig. 1(a)] and TEM [Fig. 1(b)] images. These images indicate that the product mainly consists of GaO NWs with diameter between 40 and 150 nm, and the typical lengths of these nanowires are in the range between 10 and

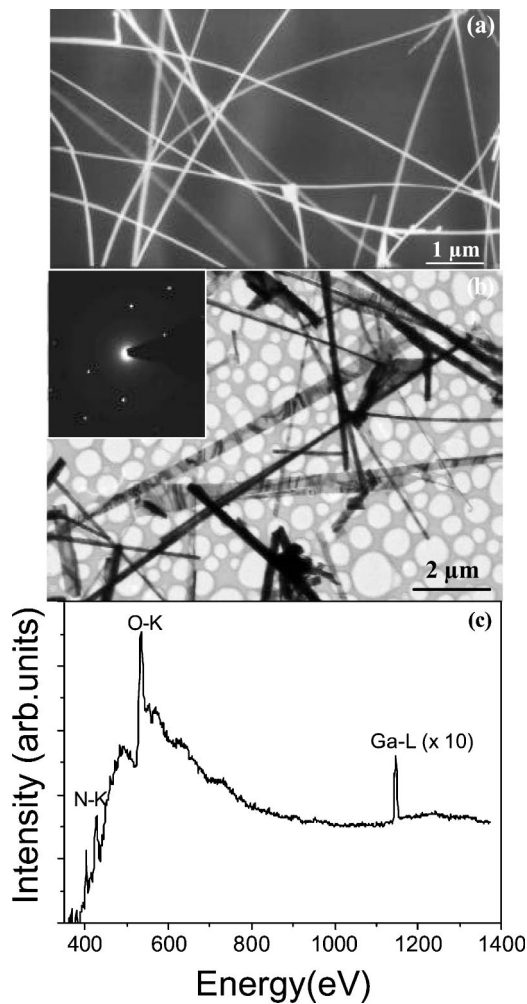


FIG. 1. General morphology of the nitrogen-doped GaO NWs. (a) SEM image and (b) TEM image. Inset shows corresponding SEAD patterns. (c) Electron energy-loss spectra of N-doped GaO NWs (sample 1).

50 μm . The selected-area electron diffraction (SEAD) analysis revealed that the as-grown GaO NWs were monoclinic crystalline gallium oxide. The composition of the N-doped GaO NWs was also analyzed using EELS and the result was shown in Fig. 1(c). Ionization edges arising from nitrogen were observed around 402.8 eV, which indicates that the nitrogen has been doped into the GaO NWs after heat treatment in flowing ammonia.

XPS is a powerful method to study the element binding state and the chemical environment in a crystal. It was used here to analyze the nitrogen dopant concentration in the GaO NWs. Figure 2 shows the XPS spectra of Ga(3*d*), N(1*s*), and O(1*s*) from samples 1–3. It is obvious from Fig. 2(a) that the peak position corresponding to Ga(3*d*) is different in the three samples, and there is a significant downshift in the binding energy of Ga(3*d*) with the increase of the nitrogen dopant, which is 20.41 eV, 20.06 eV, and 19.44 eV for samples 1–3, respectively. This result indicates that the nitrogen concentration in sample 1 is the lowest, so its binding energy is nearest to that of Ga(3*d*) of the gallium oxide (20.4 eV). With the increase of the nitrogen doping, more

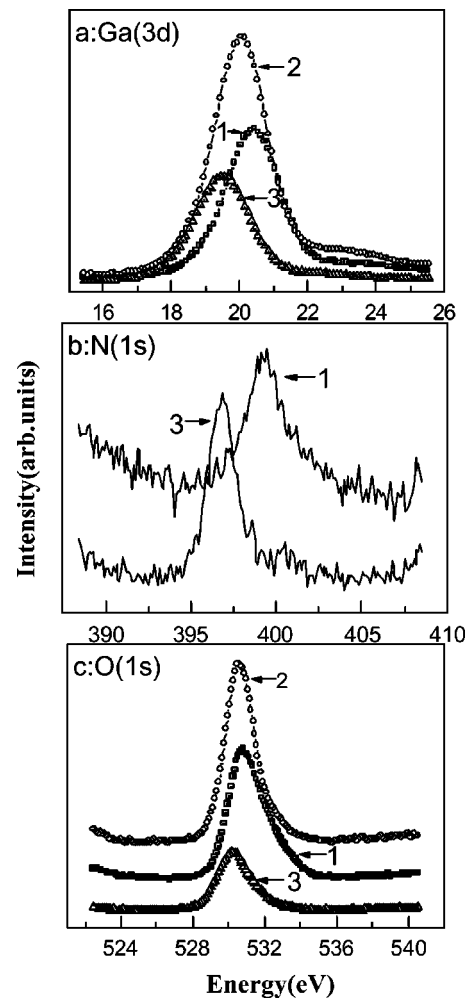


FIG. 2. The XPS spectra of Ga(3*d*), N(1*s*), and O(1*s*) for the nitrogen-doped GaO NWs.

oxygen atoms were substituted by nitrogen, and the binding energy of Ga(3*d*) decreases due to the fact that the electronegativity of nitrogen is smaller than that of oxygen. For sample 3, the binding energy of Ga(3*d*) tends to approach that of GaN (19.5 eV). Figure 2(b) shows apparently that the chemical energy shifts of N(1*s*) between samples are very large (sample 1, 399.36 eV; sample 3, 396.85 eV). This reveals that the chemical environment of nitrogen atoms in gallium oxide is affected considerably by the doping of nitrogen. Furthermore, the very broad peak of N(1*s*) spectrum from sample 1 indicates that the chemical environment of nitrogen atoms is complicated, and some kind of disorder of the nitrogen atoms may exist in the doped gallium oxide. Since the electronegativity of nitrogen is larger than that of gallium, the N(1*s*) binding energy tends to decrease with the increase of the nitrogen concentration, and it further decreased to 396.85 eV in sample 3, which approaches the value for GaN. From Fig. 2(c), the O(1*s*) binding energy at low-nitrogen doped sample 1 is near to that of gallium oxide (530.8 eV). In fact, the O(1*s*) chemical energy shifts between samples 1, 2, and 3 are small, which shows that the influence of dopant concentrations on oxygen is not so significant compared to the effect on nitrogen and gallium. Ac-

According to quantitative XPS analysis, the nitrogen dopant concentrations for samples 1, 2, and 3 are around 1.01 at. %, 1.06 at. %, and 2.60 at. %, respectively.

Our results indicate that the nitrogen concentration is mainly dominated by the treatment temperature, which implies that the doping of the nitrogen was controlled by the diffusion process. When the heat-treatment temperature is not high enough ($<700^\circ\text{C}$), nitrogen atoms are disordered in gallium oxide. However, at higher temperature, nitrogen atoms are much easier to bond with gallium atoms with more stable chemical bonds, and the gallium nitride clusters or galliumoxynitrides intermediate phase (GaO_xN_y) may appear in gallium oxide.^{15,16} For example, when the GaO NWs were heated under ammonia atmosphere (50 sccm) at 900°C for 30 min, the nitrogen concentration can be as high as 4.11 at. % in the nanowires, and apparent diffraction peaks corresponding to gallium nitride phase can be detected in XRD spectra.

For comparison, the PL spectra of the as-grown GaO NWs were measured between 10 and 300 K, as shown in Fig. 3(a). The main emission characteristic of the as-grown GaO NWs is a broad blue-green band, while no uv band was measured due to the limitation of the 325-nm excitation. The blue-green emission peaks have a blueshift with the increase of the temperature, and are peaked at 2.56 eV and 2.43 eV at 300 K and 10 K, and the full width at half maximum (FWHM) is 0.65 eV and 0.95 eV, respectively. The relative intensity increases with a decrease of the measurement temperature, in agreement with the reported results.^{12,13} The green-blue peak can in fact be decomposed into several sub-peaks, each corresponding to a defect level with a different recombination mechanism. Similar blueshift from 2.54 eV at 12 K to 2.75 eV at 300 K was also observed under excitation at 4.67 eV in a Zr-doped single crystal, which is contrary to normal expectations.⁶ The observed abnormal emission characters as a function of temperature are not yet well understood, however we think that the observed blueshift is related to the difference in the activation energies of the recombining charges at different temperatures.

Figure 3(b) shows the PL spectra for sample 1 (nitrogen concentration ~ 1.01 at. %) measured at the temperature range between 10 and 300 K. It is seen that the PL spectra are different from that of as-grown GaO NWs. First, besides the broad blue-green peaks observed in the as-grown sample, a new red peak around 1.71 eV emerges after doping, which has a blueshift and becomes more and more intense with the decrease of the temperature. Secondly, the PL intensity from sample 1 is nearly four times more intense than that of the as-grown GaO NWs. The PL spectra of the heavily doped GaO NWs with high nitrogen concentration 2.60 at. % (sample 3) were also measured in detail at the temperature range between 10 and 300 K under the same experimental condition, as is shown in Fig. 3(c). As expected, the intensity of the doping-induced red-light emission increased about ten times more than that of the as-grown GaO NWs. At 10 K, the red emission is peaked at 1.67 eV with a FWHM value around 0.5 eV. With increasing temperature, the intensity of the red emission decreases and the peak position shifts to lower energy and finally positions 1.65 eV at 300 K. This is

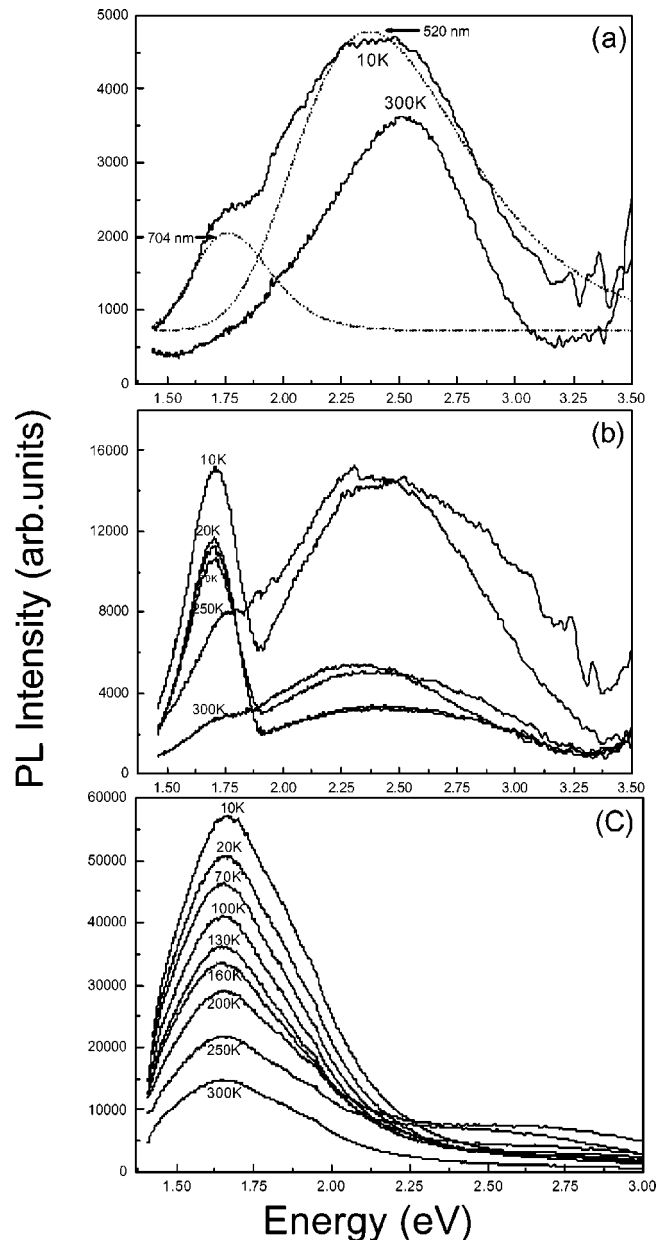


FIG. 3. PL spectra of the GaO NWs measured at temperatures between 10 and 300 K. (a) As-grown GaO NWs. Only a broad green-blue peak was observed at 300 K, while a weak red peak (around 1.76 eV) emerges at 10 K, arising from the intrinsic impurity in the as-grown GaO NWs. (b) Sample 1 (nitrogen concentration around 1.01 at. %). A novel red-light emission at 1.71 eV appears even at 300 K, which increases in intensity and has a blueshift with the decrease of the temperature. (c) Sample 3 (nitrogen concentration around 2.60 at. %). The red light emission overwhelms the green-blue bands, and its intensity is 10 times that of the as-grown GaO NWs.

in contrast to that for the blue-green bands, as seen in Fig. 3(a). The temperature dependence of the red emission of sample 3 is consistent with that of sample 1 shown in Fig. 3(b), indicating that the origin of the new red emission is the same for all doped samples. The concentrations of the doped nitrogen have a considerable influence on the red luminescence characteristic, suggesting that the nitrogen doping

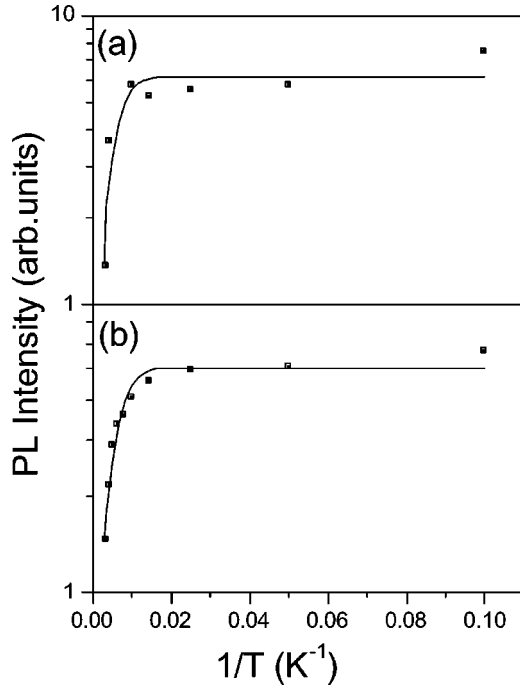


FIG. 4. Temperature dependence of PL intensity from doped GaO NWs [(a) sample 1; (b) sample 3]. Solid lines are the least-squares fitting. The parameters used for fitting are $\Delta E=0.036$ eV, $c=7.34$ for sample 1 and $\Delta E=0.034$ eV, $c=7.26$ for sample 3.

leads to the novel red emission of the GaO NWs. Comparison of the PL spectra between the as-grown and doped GaO NWs revealed that the novel red-light emission is closely related to the change of the band-gap structure of the gallium oxide crystal induced by nitrogen doping.

In order to evaluate the thermal activation energy of the novel red emission transition, the temperature dependence of the normalized emission intensity was fitted with the well-known expression¹⁷

$$I(T) = I(0) / [1 + c \exp(-\Delta E/k_B T)], \quad (2.1)$$

where c is a constant, k_B is Boltzmann's constant, $I(0)$ is the emission intensity at 0 K, while ΔE is the activation energy for the carrier involved in the recombination. The fitting results are shown in Fig. 4. The parameters used for fitting are $\Delta E=0.036$ eV, $c=7.34$ for sample 1 and $\Delta E=0.034$ eV, $c=7.26$ for sample 3. These values are almost the same for samples 1 and 3, confirming that the red emission in the doped samples has the same origin. The reported activation energy of donors due to the oxygen vacancies was at 0.03–0.04 eV (Ref. 18) in β -Ga₂O₃. In our case, ΔE is about 0.034 eV, consistent with the value of donors due to oxygen vacancies. Therefore, the obtained value of ΔE corresponds here to the activation energy of the shallow donor due to the oxygen vacancies below the conduction band. Furthermore, it indicates that the electrons trapped on the donor are involved in the red luminescence recombination.

The phosphorescence decay of sample 3 was measured under excitation from the xenon lamp of the 266-nm line. Figure 5 shows the phosphorescence-decay curves of luminescence emissions at 77 K and 300 K. Figure 5(a) reveals

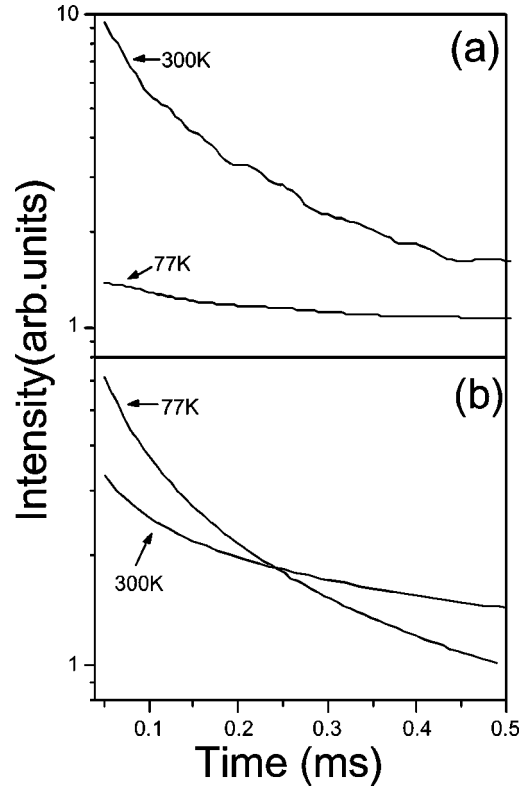


FIG. 5. The phosphorescence-decay curves of the blue- (a) and the red-light (b) emissions from sample 3 at 77 K and 300 K, respectively. The characteristic lifetime of red emission is around 136 μ s at 77 K, much shorter than that of the blue emission (457 μ s).

that the blue emission has a rather long decay with a characteristic time of 457 μ s at 77 K, which is consistent with the results of Harwig and Kellendonk.¹⁹ The characteristic lifetime of red emission is of 136 μ s at 77 K. The decay rate decreases at room temperature, that is, the tangent to the decay curve becomes steeper at 77 K compared to that at 300 K, as shown in Fig. 5(b). This indicates that the decay of the red emission is temperature-dependent. The temperature-dependent phosphorescence mechanism comprises an activated release of trapped electrons or positive holes, followed by a recombination of the electrons and positive holes. So, the phosphorescence-decay measurements on the nitrogen-doped GaO NWs revealed that the red-light emission comes from the electron-hole recombination. As mentioned above, the electron on the donor due to oxygen vacancies is involved in the red luminescence recombination. So, the other carrier involved in the recombination will be related to the nitrogen doping (N^{-3} substitutes for O^{-2}). When nitrogen ions are doped into the lattice and substituted for oxygen, the nitrogen dopants can generate acceptor levels in the band gap of gallium oxide. Therefore, it is proposed that the novel red-light emission originates from the recombination of an electron trapped on a donor due to oxygen vacancies and a hole trapped on an acceptor due to the nitrogen dopant. In order to prove this hypothesis, the decay time and the luminescence spectra of the red-light emission were calculated using the donor-acceptor pair (DAP) model proposed by Thomas *et al.*,²⁰ under consideration of the thermal quench-

ing effect. In $\beta\text{-Ga}_2\text{O}_3$, the reported donor concentration due to oxygen vacancies was $n_D \approx 10^{18} \text{ cm}^{-3}$. As to the nitrogen-doped GaO NWs, the nitrogen dopant concentration is about 2.60 at. % for sample 3 as analyzed by XPS. However, XPS is a surface analysis method and the dopant concentration decreases inside of the nanowires, so the reasonable nitrogen concentration at equilibrium is estimated to be 10^{19} cm^{-3} . Therefore, the acceptor concentration due to the nitrogen doping greatly exceeds the donor concentration in the nitrogen-doped GaO NWs.

III. THEORETICAL CALCULATION AND DISCUSSION

Thomas *et al.*²⁰ investigated the kinetics of radiative recombination of acceptors and donors in S/Si-doped GaP by comparison of the experimental decay behavior with the theoretical calculations, and put forward a DAP model to explain the observed luminescence spectra. The present case is very similar to that of the doped GaP, so their model can be used to simulate the emission characteristics and explain the time decay of the novel emission due to N doping in GaO NWs, with some modifications made to fit our case. According to DAP theory, the minority carriers (the donors in our case) are supposed to be surrounded by a random distribution of majority carriers, e.g., the acceptors at distance r from a donor. The main approximation of the model was that all donors and acceptors are assumed to be neutral. Tunnel recombination will occur from an electron at a donor site with a hole at an acceptor site, and a photon is emitted with energy,^{20,21}

$$E = E_g - (E_d + E_a) + E_c \pm nE_{\text{phonon}}, \quad (3.1)$$

where E_g is the band gap, E_d and E_a are the ionization energies for the donor and acceptor respectively, and E_{phonon} is the phonon energy involved in the radiative transition, with $n=0,1,2,\dots$. The term $E_c = e^2/4\pi\epsilon r$ corresponds to the Coulombic interaction between an ionized donor and acceptor.

The recombination probability for a donor-acceptor pair with separation r is expressed as²⁰

$$W(r) = W_{\text{max}} \exp(-2r/R_d), \quad (3.2)$$

where R_d is the Bohr radius of the shallowest defect. Equation (3.2) holds when one defect is much shallower than the other. In the case of nitrogen-doped GaO NWs, the acceptors due to the nitrogen doping are of a deep energy level, the ionization energies of the acceptors are much larger than that of the donors, and the Bohr radius R_d for a donor in $\beta\text{-Ga}_2\text{O}_3$ is around 1.8 nm. For a given configuration of acceptors at positions r and a donor at the origin, the average of the probability for an electron on the donor sites is denoted by $\langle Q(t) \rangle$,²⁰

$$\langle Q(t) \rangle = \exp \left[4\pi n \int_0^\infty \{ \exp[-W(r)t] - 1 \} r^2 dr \right]. \quad (3.3)$$

As we know, the temperature has a large influence on the luminescence, and an electron on a donor or a hole on an acceptor can be detrapped with an increase of temperature.

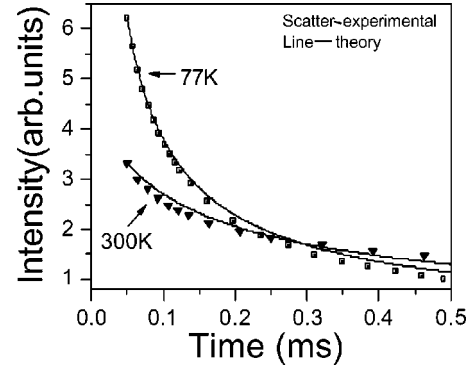


FIG. 6. The theoretical calculation (line) of the time decay of the red-light emission using Eq. (3.4) at 77 K and 300 K, and compared with the measured data (scatter). The concentration of the acceptors $n = 2 \times 10^{19} \text{ cm}^{-3}$. (a) $W_{\text{max}} = 6 \times 10^4 \text{ s}^{-1}$; (b) $W_{\text{max}} = 6 \times 10^6 \text{ s}^{-1}$.

However, the thermal quenching effect was not considered in the above treatment. Therefore, a new term will be included in Eq. (3.3) to describe the temperature dependence of the total luminescence intensity. In the nitrogen-doped GaO NWs, the electron is more easily detrapped than the hole because the activation energy of the acceptor due to nitrogen doping is much larger than that of the donor. So one needs only to consider the thermal quenching effect on the donor. Therefore, the intensity $I(t, T)$ of light emitted at time t and temperature T is given by

$$\begin{aligned} I(t, T) &= \frac{1}{1 + c \exp(-E_d/k_B T)} \frac{d}{dt} \langle Q(t) \rangle \\ &= \left\{ \frac{4\pi n}{1 + c \exp(-E_d/k_B T)} \right. \\ &\quad \times \int_0^\infty W(r) \exp[-W(r)t] r^2 dr \left. \right\} \\ &\quad \times \left\{ \exp \left[4\pi n \int_0^\infty \{ \exp[-W(r)t] - 1 \} r^2 dr \right] \right\}, \end{aligned} \quad (3.4)$$

where n is the concentration of the majority carriers, and in our case it is referred to acceptors. For given $W(r)$, this treatment is a typical statistical problem in the limit of a large ratio of acceptor/donor concentrations, as it is in our case.

The time decay of the red luminescence can be calculated using Eq. (3.4), and there are two variable parameters: the acceptor concentration and the maximum recombination probability W_{max} . Based on the above-mentioned formulas, we calculated the decay time of luminescence for sample 3. Figure 6 shows the comparison of calculated (line) and experimental (scatter) measurements for the time decay of the red emission at 77 K and 300 K. The acceptor concentration used for calculation is $n = 2 \times 10^{19} \text{ cm}^{-3}$, which results in $W_{\text{max}} = 6 \times 10^6 \text{ s}^{-1}$ at 77 K and $W_{\text{max}} = 6 \times 10^4 \text{ s}^{-1}$ at 300 K, respectively. It can be seen the calculation results agree pretty well with the experiment data at 77 K, and only

a little deviation occurs at 300 K. All the results indicate the red emission follows a power-law decay with hyperbolic kinetics, whose mechanism comprises an activated release of trapped electrons or positive holes, followed by a bicarrier-type recombination of the electrons and positive holes. Therefore, the power-law decays are quite sensitive to changes of temperature, excitation density, and excitation energy.

The calculation of the temperature-dependent luminescence spectra was described as follows. According to Thomas *et al.*,²⁰ if the electron on the donor recombined with a hole on an acceptor a distance r_1 away, the energy would be given in lowest order by Eq. (3.1), independent of the other acceptors. This permits one to calculate the total emission spectrum. The intensity $J_E(t)$ at energy E is given by

$$J_E(t) = W(r_1) \exp[-W(r_1)t] \exp\left[-\sum_{j \neq 1} W(r_j)t\right]. \quad (3.5)$$

The observed decay time should be the ensemble average of Eq. (3.5) over all possible positions of the other donors, which is the same as Eq. (3.3),²⁰

$$\langle J_E(t) \rangle = W(r_1) \exp[-W(r_1)t] \langle Q(t) \rangle. \quad (3.6)$$

When considering the thermal quenching effect, the intensity $I(t, T)$ at energy E time t , and temperature T is given by

$$I_E(t, T) = \frac{4\pi n(e^2/4\pi\epsilon)^3}{E_c^4(1+c \exp(-E_d/k_B T))} \langle J_E(t) \rangle. \quad (3.7)$$

Combining Eqs. (3.1), and (3.2) into Eq. (3.7), the intensity $I_E(T)$ of the total luminescence emission is expressed as follows:

$$I_E(T) = \int_0^\infty \left(\frac{4\pi n(e^2/4\pi\epsilon)^3}{E_c^4[1+c \exp(-E_d/k_B T)]} \right) \times W_{\max} \left\{ \exp\left[-\frac{2e^2}{4\pi\epsilon E_c R_d}\right] - W_{\max} t \exp\left(-\frac{2e^2}{4\pi\epsilon E_c R_d}\right) \right\} \langle Q(t) \rangle dt. \quad (3.8)$$

Observation of luminescence from gallium oxide has been studied widely and only uv, blue-, and green-light emissions were reported. Harwig *et al.*¹⁹ showed that samples annealed in a reduction atmosphere favor the formation of oxygen vacancies and blue emission was enhanced, while samples heated in an O₂ atmosphere favor the formation Ga vacancies, which show a dominant green emission. It was proposed that the blue-green emissions from gallium oxide crystal originate from a tunnel recombination of an electron on a donor formed by oxygen vacancy (V_O) with a hole on the acceptor formed by a gallium-oxygen vacancy pair (V_O, V_{Ga}). Those experimental results confirmed that the blue-light emission originates from the recombination of the

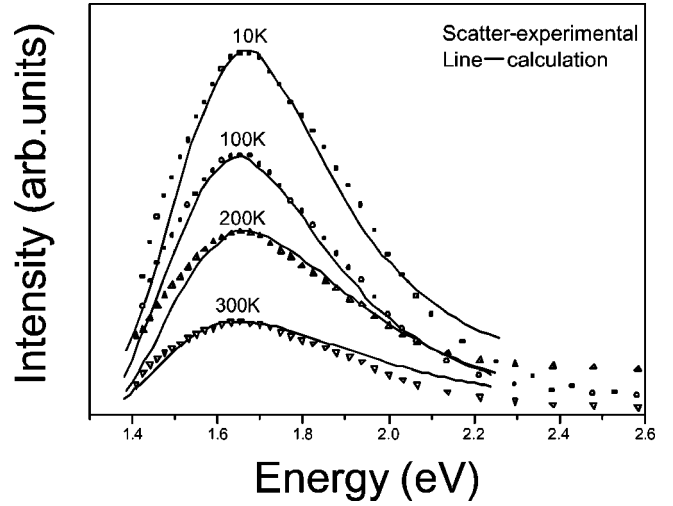


FIG. 7. Theoretical simulation of the temperature dependence of luminescence spectra for sample 3 for 10, 100, 200, and 300 K, respectively. The calculated PL curves (solid lines) were compared with the corresponding experimental spectra (dashed lines) in Fig. 3(c), and both agree with each other. $n = 2 \times 10^{19} \text{ cm}^{-3}$, $c = 7.4$, and $W_{\max} = 1 \times 10^7$, 7×10^5 , 2×10^5 , and $6 \times 10^4 \text{ s}^{-1}$ at 10, 100, 200, and 300 K, respectively.

trapped excitons formed by an electron and a hole. For GaO NWs synthesized at high temperature, large quantities of oxygen vacancies (V_O) and gallium-oxygen vacancy pair (V_O, V_{Ga}) (Ref. 22) can be easily produced. The blue-green PL feature of GaO NWs in our case is consistent with the model mentioned above. However, red-light emission due to doping in gallium oxide was not yet reported. The red luminescence spectra for sample 3 were calculated using Eq. (3.8), which proved to be complicated. At a limited temperature, the photons emitting from the recombination of electrons and holes will interact with lattice vibration via emitting or absorbing phonons. The higher the temperature, the larger the interaction, which will cause broadening to the luminescence spectra. PL emission spectra at different temperatures were calculated, and comparison of the calculated results (line) with the experiment data [scatter, the same as in Fig. 3(c)] was shown in Fig. 7. The parameters $W_{\max} = 1 \times 10^7$, 7×10^5 , 2×10^5 , and $6 \times 10^4 \text{ s}^{-1}$ were used for calculation at 10, 100, 200, and 300 K, respectively. It can be seen that there is very good agreement between the observed and calculated spectra. In principle, the acceptor ionization energy can be deduced from the energy position of the no-phonon line and the band gap E_g of the β -Ga₂O₃.

For heavily doped semiconductors, the band gap can be reduced due to the formation of dopant subbands between the band gap.²³ For sample 3, the nitrogen dopant concentration is up to 10^{19} cm^{-3} , so the acceptor induced by nitrogen doping will form a dopant subband in the band gap and decrease the band gap of β -Ga₂O₃, which leads to the red-shift of the red emission with the increases of the nitrogen concentration. It is noted that a weak red emission peak around 1.76 eV appeared at 10 K but is absent at 300 K in the as-grown GaO NWs, shown in Fig. 3(a). Such a red emission in the as-grown GaO NWs may arise from impuri-

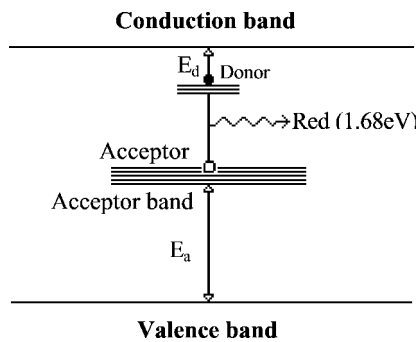


FIG. 8. Schematic depiction of the novel red-light emission process induced by nitrogen doping in GaO NWs. It is revealed the nitrogen doping induced a hole trap in the acceptor, which will recombine with electron trapped at the donor due to oxygen vacancy, resulting in red-light emission.

ties, because it is not surprising that any pure material contains inevitably some impurities.

Our theoretical calculations are very consistent with the experiment data for the time decay and temperature dependence of the luminescence spectra for sample 3, suggesting that the red-light emission in nitrogen-doped GaO NWs originates from the recombination of an electron trapped on a donor due to oxygen vacancies and a hole trapped on an acceptor due to nitrogen doping. The nitrogen doping generates deep acceptor levels in the band gap of gallium oxide, and the position of the doping-induced subbands is about at the center of the band gap, which is depicted in Fig. 8. The electron trapped on a donor and the hole trapped on an acceptor will recombine radiatively, emitting a photon with wavelength around 1.67 eV. With the increase of temperature, the electron will detrapp from a donor to the conduction band, whereas the hole will detrapp from an acceptor to the

valence band. So the red-light emission will decrease and can be quenched considerably with increasing temperature.

IV. CONCLUSION

Nitrogen was doped into GaO NWs by post-annealing the as-grown GaO NWs in flowing ammonia. The concentration of the doped nitrogen in GaO NWs is dominated mainly by the treatment temperature. The photoluminescence (PL) spectra were measured for both nitrogen-doped and as-grown GaO NWs at temperature ranging between 10 and 300 K. The PL measurements revealed a novel red-light luminescence emission induced by nitrogen doping in the gallium oxide. The emission intensity of red-light emission increases with decreasing temperature and the peak position shifts towards lower energy with the increase of the nitrogen concentration doped into the GaO NWs. Phosphorescence-decay and temperature-dependent luminescence spectra of the red emission were calculated based on a donor-acceptor-pair (DAP) model, which is in excellent agreement with the experimental data, and revealed that the observed novel red-light emission originates from the recombination of an electron trapped on a donor due to oxygen vacancies and a hole trapped on an acceptor due to nitrogen doping. The peculiar intensive red luminescence from nitrogen-doped GaO NWs will make the nitrogen-doped GaO NWs excellent candidates for optoelectronic nanodevice applications.

ACKNOWLEDGMENTS

This project is financially supported by the National Natural Science Foundation of China (Grant Nos. 50025206, 60071014, 20151002), and national 973 projects (No. 2002CB613505, MOST). D.P.Y. is supported by the Cheung Kong.

*Corresponding author. Email address: yudp@pku.edu.cn

¹H.Z. Zhang, Y.C. Kong, Y.Z. Wang, X. Du, Z.G. Bai, J.J. Wang, and D.P. Yu, *Solid State Commun.* **109**, 677 (1999); T. Miyata, T. Nakatani, and T. Minami, *J. Lumin.* **87**, 1183 (2000); R. Bene and Z. Pinter, *Vacuum* **61**, 275 (2001).

²L. Zisen, G. Cornelisde, and H.M. Jagadeesh, *Appl. Phys. Lett.* **77**, 3630 (2000).

³A.P. Alivisatos, *Science* **271**, 933 (1996).

⁴E.W. Wong, P.E. Shechan, and C.M. Lieber, *Science* **277**, 1971 (1997).

⁵Z.W. Pan, Z.R. Dai, and Z.L. Wang, *Science* **291**, 1947 (2001).

⁶L. Binet and D. Gourier, *J. Phys. Chem. Solids* **59**, 1241 (1998).

⁷E.G. Villora, T. Atou, T. Sekiguchi, and T. Sugawara, *Solid State Commun.* **120**, 455 (2001).

⁸M. Ogita, K. Higo, Y. Nakanishi, and Y. Hatanaka, *Appl. Surf. Sci.* **175**, 721 (2001).

⁹J. Frank, M. Fleischer, and H. Meixner, *Sens. Actuators B* **48**, 318 (1998); J. Frank, M. Fleischer, H. Meixner and A. Feltz, *ibid.* **49**, 110 (1998).

¹⁰N. Ueda, H. Hosono, R. Waseda, and H. Kawazoe, *Appl. Phys. Lett.* **70**, 3561 (1997); **71**, 933 (1997).

¹¹L. Binet and D. Gourier, *Appl. Phys. Lett.* **77**, 1138 (2000).

¹²C.H. Liang, G.W. Meng, G.Z. Wang, Y.W. Wong, and L.D.

Zhang, *Appl. Phys. Lett.* **78**, 3202 (2001).

¹³D.P. Yu, J.L. Bubendorff, J.F. Zhou, Y.L. Wang, and M. Troyon, *Solid State Commun.* **124**, 417 (2002).

¹⁴X.C. Wu, W.H. Song, W.D. Huang, M.H. Pu, B. Zhao, Y.P. Sun, and J.J. Du, *Chem. Phys. Lett.* **328**, 5 (2000).

¹⁵W.S. Jung, *Mater. Lett.* **57**, 110 (2002).

¹⁶C.M. Balkas and R.F. Davis, *J. Am. Ceram. Soc.* **79**, 2309 (1996).

¹⁷K.W. Mah, E.M. Glynn, J. Castro, J.G. Lunney, J.P. Mosnier, D.O. Mahony, and M.O. Henry, *J. Cryst. Growth* **222**, 497 (2001).

¹⁸M.R. Lorenz, J.F. Woods, and R.J. Gambino, *J. Phys. Chem. Solids* **28**, 403 (1967).

¹⁹T. Harwig, and F. Kellendonk, *J. Solid State Chem.* **24**, 255 (1978).

²⁰D.G. Thomas, J.J. Hopfield, and W.M. Augustyniak, *Phys. Rev.* **140**, A202 (1965).

²¹D.G. Thomas, M. Gershenson, and F.A. Trumbore, *Phys. Rev.* **133**, A269 (1964).

²²V.I. Vasiltsev, Y.M. Zakharko, and Y.I. Prim, *Ukr. Fiz. Zh. (Russ. Ed.)* **33**, 1320 (1988).

²³J.I. Pankove, *Optical Processes in Semiconductors* (Princeton University Press, Princeton, NJ, 1973), p. 27.